Calhoun
Institutional Archive of the Naval Postgraduate School

Calhoun: The NPS Institutional Archive

DSpace Repository

Faculty and Researchers | Faculty and Researchers' Publications

2003-06

Control of Compressible Dynamic Stall Using Microjets

Shih, C.; Beahn, J.; Krothapalli, A.; Chandrasekhara, M.S.

C. Shih, J. Beahn, A. Krothapalli and M.S. Chandrasekhara, "Control of Compressible Dynamic Stall Using Microjets", ASME Fluids Engineering Meeting, Honolulu, HI, June 2003.
https://hdl.handle.net/10945/50035

Downloaded from NPS Archive: Calhoun

http://www.nps.edu/library

Calhoun is the Naval Postgraduate School's public access digital repository for research materials and institutional publications created by the NPS community. Calhoun is named for Professor of Mathematics Guy K. Calhoun, NPS's first appointed -- and published -- scholarly author.

Dudley Knox Library / Naval Postgraduate School
411 Dyer Road / 1 University Circle
Monterey, California USA 93943

Proceedings of ASME FEDSM'03
4th ASME_JSME Joint Fluids Engineering Conference
Honolulu, Hawaii, USA, July 6-10, 2003

FEDSM2003-45627

CONTROL OF COMPRESSIBLE DYNAMIC STALL USING MICROJETS

C. Shih, J. Beahn, and A. Krothapalli
Department of Mechanical Engineering
FAMU-FSU College of Engineering
Tallahassee, FL 32310

M.S. Chandrasekhara
Department of Aeronautics and Astronautics
Naval Postgraduate School
Monterey, CA 93043

ABSTRACT

Control of the dynamic stall process of an NACA 0015 airfoil undergoing periodic pitching motion is investigated experimentally in a high-speed wind tunnel facility. Multiple microjet nozzles distributed uniformly in the first 15% chord from the airfoil's leading edge are used for the control. Point Diffraction Interferometry (PDI) technique is used to characterize the control effectiveness, both qualitatively and quantitatively. The microjet control has been found to be very effective in suppressing both the emergence of the dynamic stall vortex and the associated massive flow separation at the entire operating range of angles of attack. At the high Mach number case (M=0.4), the use of microjets appears to eliminate the shock structures that are responsible for triggering the shock-induced separation, establishing the fact that the use of microjets is effective even in controlling dynamic stall with a strong compressibility effect. In general, microjet jet control has an overall positive effect in terms of maintaining leading edge suction pressure and preventing flow separation.

Keywords: dynamic stall, microjet control, compressible flow, unsteady aerodynamics, separated flow

INTRODUCTION

The dynamic stall process on a helicopter rotor blade is initiated by the unsteady boundary-layer separation near the airfoil's leading edge. During a rapid pitch-up motion, vorticity production is greatly enhanced by the presence of a favorable pressure gradient at the leading edge. At the same time, vorticity accumulates locally due to the slowdown of downstream convection process caused by an adverse pressure gradient and a local boundary-layer flow reversal further downstream. The accumulation process is eventually interrupted by a sudden emergence of unsteady flow separation and the subsequent eruption of the accumulated vorticity into the outer flow. Consequently, it initiates a sequence of spontaneous events such as local viscous/inviscid boundary-layer interaction, formation and convection of large energetic and, finally the "stall" and all associated adverse effects. Thus, in order to control the dynamic stall process, a better physical understanding of the unsteady boundary-layer separation is necessary.

A detailed theoretical description of the unsteady separation process was first made by van Dommelen and Shen (VDS)[1] using an innovative Lagrangian approach. In short, the process is initiated by a local flow reversal as the result of the adverse pressure gradient. The fastest reversing particles quickly collide with the slower moving particles ahead of them. This results in a local eruption of the particles away from the wall and initiates the separation process. Unlike the traditional shear layer instability mechanism, which selectively amplifies random perturbations in the initial region to develop into organized vortical structures, the deformation triggered by the VDS interaction provides a deterministic perturbation to the local vorticity distribution. After this sudden distortion, the local vorticity arrangement is highly unstable and quickly rolls up into a large dynamic stall vortex (see figure 1)[2]. Once generated, the energetic vortical structure is extremely robust and is difficult, if not impossible, to control. Therefore, any effective control of the dynamic stall process has to be carried out before the formation of the vortex. That is, one has to control the unsteady separation process as described by the VDS model in order to prevent or alleviate the sudden eruption of vorticity from the wall.

There are many ways to implement control on the dynamic stall process to produce the desirable effect. Only active control strategies will be considered here since, unlike passive control elements, they can be switched on and off instantly, therefore, they will not degrade the operational performance when they are not needed. For example, Wang[3] used uniform suction near the separation region and his computational results show that the formation of the dynamic stall vortex can be significantly delayed or even eliminated. However, the power required to achieve effective suction makes this proposal

 Copyright © 2003 by ASME

Downloaded From: http://proceedings.asmedigitalcollection.asme.org/ on 09/30/2016 Terms of Use: http://www.asme.org/about-asme/terms-of-use

unrealistic. Lewington et al.[4] used Air-Jet Vortex Generator (AJVGs) to generate multiple vortical structures that are capable of energizing the boundary layer in order to delay boundary layer separation. They have shown that stall can be delayed with an increase of lift and a decrease of drag. However, their results have been limited to quasi-steady conditions only. In this program, we propose the implementation of a distributed, multiple microjet control system to provide high-energy perturbations for the unsteady separation control. The microjet control unit is similar to the system we used successfully in the control of supersonic impinging jets[5]. Groups of these microjet nozzles (of the order of one hundred microns in diameter) will be distributed uniformly near the leading edge of the airfoil. Different from the AJVGs, these microjets will be driven with higher plenum pressure so that they can achieve very high momentum. Due to their much smaller size, it is expected that these microjets will have smaller amount of total blowing mass flux as the AJVGs system. However, their higher momentum and close spacing provide an advantage to achieve the effective separation control as will be discussed in the next section. A second advantage of using the microjets is that they can be produced in large quantity and selectively patterned by taking advantage of existing microfabrication techniques. Therefore, it is possible to fabricate an assembly of a very large number of microjets with desirable spatial distribution for multiple point control. Finally, microfabricated sensors can be packaged with the control unit for multiple-point signal detection and control activation. This makes in-situ active flow control possible.

Compressibility effect, which can appear at free-stream Mach number as low as M=0.2, can have significant effects on the initiation of the dynamic stall. Increased Mach number reduces the capability of boundary layer to withstand adverse pressure gradient[6], leading to early separation and dynamic stall. On the other hand, a supersonic bubble can also form at the leading edge and the associated shock/boundary layer interaction can trigger the premature release of vorticity and a reduction of peak lift coefficient[7,8]. The bursting of the separation bubble at higher angles of attack will lead to the onset of the dynamic stall process. It has also been shown that[9] increasing Reynolds numbers and the tripping of the leading edge boundary layer can alleviate this effect. Consequently, higher suction pressure peak can be sustained and the dynamic stall is delayed to higher angles of attack. We believe that similar effect can be achieved using the proposed microjet control system. It is speculated that the spatially distributed streamwise counter-rotating vortex pairs generated by the presence of multiple microjets can greatly enhance momentum transfer between the outer flow and the boundary layer. This should enable the boundary layer to withstand very steep adverse pressure gradient and result in the delay of flow separation and the dynamic stall process. Although this has not been confirmed experimentally at high Mach numbers, we also propose that VDS-type unsteady interaction process, as described earlier, is responsible for the massive vorticity eruption at higher Mach numbers. Therefore, a timely ejection of the accumulated vorticity inside the separation bubble by microjet control system should also be effective even when the compressibility effect is important.

EXPERIMENTAL SETUP

The current experiments were conducted at the Compressible Dynamic Stall Facility (CDSF) at the NASA Ames Research Center Fluid Mechanics Laboratory in Moffett Field, California. The CDSF is a facility specifically designed for studying the phenomena of dynamic stall over a range of freestream Mach numbers and reduced frequencies. Inside the test section, the airfoil is held between two 2.54 cm thick metal windows using tangs. Optical quality glass inserts in the windows, allow light to pass through the test section around the airfoil making direct visualization possible. For a more detailed description of the facility reference can be made to Carr and Chandrasekhara[10].

Point Diffraction Interferometry (PDI) is a non-invasive optical technique that measures changes in the index of refraction due to density changes in the compressible flow field. This technique utilizes the ability of a point discontinuity (a pinhole in the present case) to diffract a portion of incident light into a spherical wave front such that it can function as a point source of light itself. In the present system, a single Nd-YAG laser beam is collimated and expanded through a microscope objective lens and directed through the test section using a high quality parabolic mirror. A second parabolic mirror refocuses the light to the diffraction plate via a modified Z-type Schlieren configuration[8].

The current PDI plate is a holographic plate that consists of a diffraction pinhole centered in the semi-transparent film plate. A portion of the beam passes through the plate with controlled level of attenuation. On the other hand, the light passing through the center hole creates a spherical diffraction wave that acts as the reference beam for the interferometry effect. A fringe pattern is generated when the reference beam (through center hole) interacts with the attenuated light passed through the other area of the plate. The interference pattern is projected on an ASA 3000 Polaroid film for image recording.

Selected Polaroid photographs were digitized at a resolution of 1200 dpi to allow for accurate image recognition and fringe counting. A detailed description on the fringe processing and data interpretation can be found in Chandrasekhara et al.[8]

The testing model is an NACA 0015 airfoil with a chord of 7.62 cm. Two flow Mach numbers, M=0.3 and 0.4, were used, while the higher Mach number case corresponded to flow with strong compressibility effects. The test Reynolds number is 1.1×10^6 at a Mach number of 0.3. The non-dimensional pitch rate was varied between k=0.05 and k=0.10. The angle of attack was varied following the function $\alpha=10+10\sin(\omega t)$ for the majority of the tests, but selected cases were obtained for $\alpha=10+5\sin(\omega t)$.

A total of over 400 microjets, with a diameter of 400 μm, placed in an aligned pattern covering the upper nose region from the leading edge to about 12% chord length. The pressure inside the plenum cavity of the airfoil was measured at the extension where the air enters the airfoil outside the testing rig. This was measured using a Weston Aerospace DPM7885 precision pressure module. The pressure loss between the extension where the pressure is measured during experimentation and the plenum has been found experimentally for each microjet setup. These microjets were operated at a plenum pressure between 15 and 62 psia but was typically run at 21.7 psia unless specified otherwise. The mass injection rate

Copyright © 2003 by ASME

Downloaded From: http://proceedings.asmedigitalcollection.asme.org/ on 09/30/2016 Terms of Use: http://www.asme.org/about-asme/terms-of-use

operated at this condition was 0.03 kg/s, corresponding to a blowing momentum coefficient of approximately 0.01.

RESULTS AND DISCUSSION

Interpretation of Interferograms

The interferograms obtained from the corresponding flow conditions contain information that is both qualitative (as flow visualization) and quantitative in nature. Using image digitization and fringe-counting scheme, these images can yield many useful quantities such as the surface pressure distribution as described in the introduction section. In the following, we are going to first address the qualitative observations that provide a better understanding of the flow physics related to the emergence of dynamic stall.

Figure 1 is a typical interferogram image taken at the condition of M=0.3, k=0.10, and α=18^o. This image exemplifies many important features of the flow dynamics of the airfoil undergoing pitching-up motion. The first prominent feature is the existence of the stagnation bubble near the leading edge on the lower surface. This region can be identified as where the local fringe circles around and reconnects with the airfoil's surface in the lower left-hand portion of the image. The stagnation point can be identified at the center of this stagnation bubble where the pressure is a local maximum.

Another interesting aspect is the concentration of fringes near the leading edge indicating the existence of a large density (or pressure) gradient due to the rapid acceleration of the flow over the airfoil's nose. These local fringes also form a recirculated pattern as they emerge from the airfoil's surface

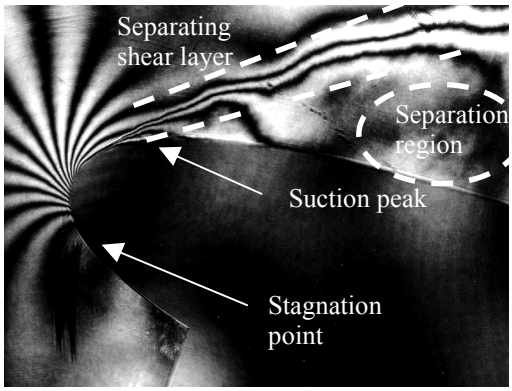

Figure 1. Point Diffraction Interferogram, no Control, M=0.3, k=0.10, and α=18^o

and circles around to reconnect with the surface again. This pattern is due to the existence of a locally minimum pressure near the airfoil's nose. In this sample image the peak fringe number counted is 8, which corresponds to a local pressure of 85.9 kPa. The rapid acceleration of flow from stagnation to a very high speed is responsible for generating the local suction pressure near the airfoil nose, thus the creation of lift. Also notice the existence of a large separation region downstream from the leading edge. This condition does not appear in every case but only in cases where massive separation has dominated due to the emergence of the catastrophic stall. Inside the separation region, no obvious fringe pattern can be observed due to the turbulent nature of the flow. A relatively flat pressure distribution is expected within this area.

Microjet Control, M=0.3

Figures 2(a)-(c) show three representative interferograms for the case of M=0.3 and k=0.10 without control. This sequence shows the reattachment of the separation region as the airfoil pitches down from high to low angles of attack. The first two images show total flow separation with a detached shear layer away from the airfoil. In figure 2(b), the appearance of a closed fringe region above the airfoil in the center of picture might be indicative of the release of a vortex from the leading edge.

In figure 2(c), the separated shear layer seems to reattach back to the surface. The increase of the number of the fringes suggests the increase of suction pressure near the leading edge and the recovery of lift. An interesting observation is the bending of the reattaching fringes when they approach closely to the airfoil surface. They tend to curve toward downstream and align parallel to the surface. As explained before, this is due to the non-uniform temperature inside the boundary layer, the fringes (constant density lines) are actually aligned closely with constant temperature lines not constant pressure lines. On the other hand, this local fringe bending makes the identification of the edge of the boundary layer easier (figure 2(c)).

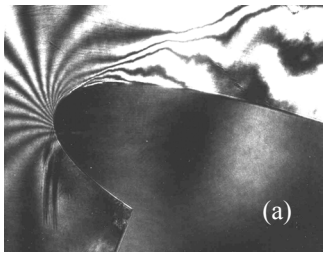

α=19.9^o upward

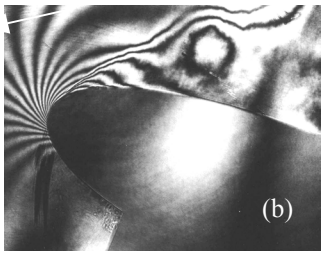

α =19.0^o downward

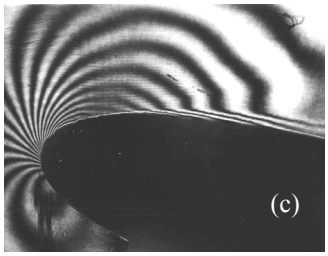

α =13.1^o downward

Figure 2. Flow sequence of a pitching airfoil, M=0.3, k=0.10, without control

Figures 3(a)-(c) show corresponding cases with microjet control (with a control pressure of 21.7 Psia.) The microjet streams can be clearly seen in the upper leading edge region.

Copyright © 2003 by ASME

Downloaded From: http://proceedings.asmedigitalcollection.asme.org/ on 09/30/2016 Terms of Use: http://www.asme.org/about-asme/terms-of-use

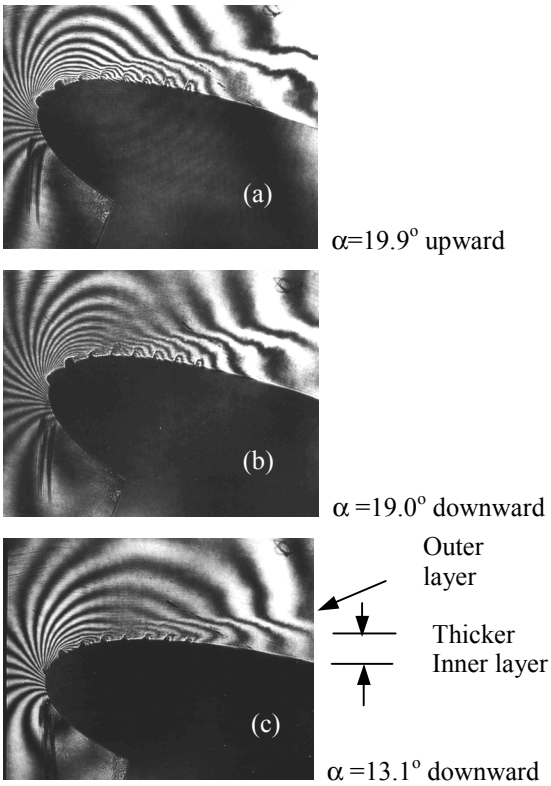

Figure 3. Flow sequence of a pitching airfoil, M=0.3, k=0.10, with control (control pressure 21.7psia)

The presence of these jet streams distorts the local fringe patterns, as one would expect from the flowfield of jet in a crossflow. Amazingly, the leading edge flow appears to remain attached when the microjet control is turned on. The increase of the number of the interference fringes near the leading edge is indicative of the fact that lower suction pressure is maintained near the nose if the microjet control is used. Qualitatively, one can conclude that the microjet control is extremely effective in eliminating the massive flow separation.

Two-Layer Structure With Control

On the other hand, these images also show that, with control, the viscous boundary layer appears to be thicker (see figure 3(c) as an example) when compared to an attached case without control (figure 2(c)). This is expected since a significant amount of fluid is being displaced away from the boundary layer due to the blowing of the microjet. Also, with control, the fringes align almost normal to the airfoil's surface instead of parallel to it, as is the case without control. This could be explained by realizing that the activation of control have generated many locally separated flow regions behind these microjets. These separated regions are highly turbulent with strong mixing characteristics, yet they are small enough to not trigger a massive separation. The culmination of these small-scale separated regions can lead to the thickening of the boundary layer. Also, one would expect that the temperature is reasonably uniform inside the thickened layer accompanied with a more uniform density profile. Therefore, constant density lines (fringes) are expected to coincide with constant pressure lines, which are aligned normal to the airfoil's surface according to the boundary layer theory. On the other hand, a sharp discontinuity of the slope of the local fringe can be seen between the thick inner layer and the outer flow. This suggests the existence of another thin outer layer separating the external flow stream from the inner viscous layer. The seemingly streamwise alignment of fringes inside this outer layer suggests the existence of a substantial vorticity gradient across the layer, the characteristic of the presence of a strong shear. It is reasonable to believe that this thin outer layer originates from the leading edge vorticity layer as it is displaced by the outward blowing microjets. Being moved away from the surface, this vorticity layer can now convect effectively downstream to prevent the significant local accumulation that might lead to the subsequent emergence of dynamic stall. The effective release of vorticity by displacing it away from the surface appears to be one of the major mechanisms why the microjet control scheme works.

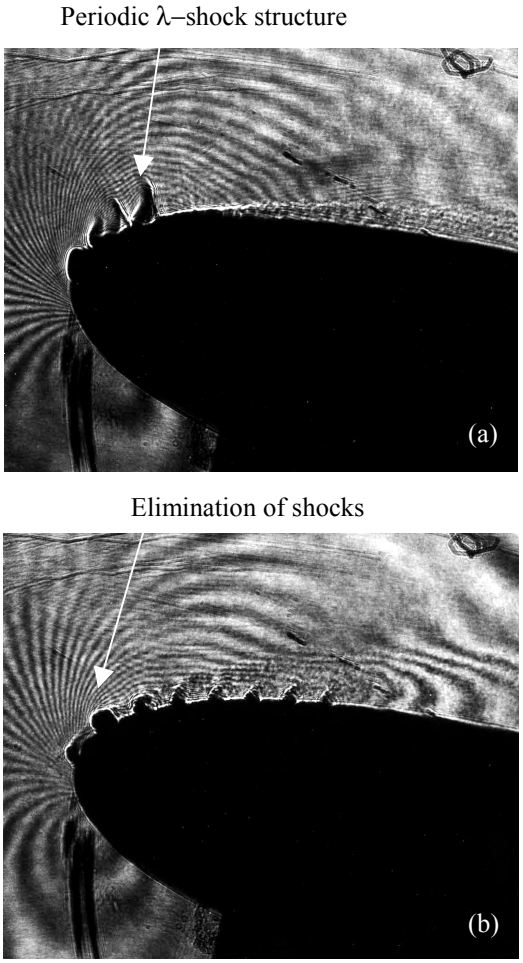

(a) No Control (b) With Control (30 psia)

Figure 4. Effect of microjet control on dynamic stall, M=0.4, k=0.05, α=12.5°

Microjet Control, M=0.4

Upon increasing the freestream Mach number to 0.4 a portion of the flow over the airfoil reaches supersonic speeds, as exemplified by the presence of shocks in Figure 4(a). These shocks only exist through a small range of angles of attack from $\alpha=12.5^o$ to $\alpha=14.6^o$. However, they play a significant role in the initiation of the dynamic stall. Due to the presence of an even stronger adverse pressure gradient across a shock, the

Copyright © 2003 by ASME

Downloaded From: http://proceedings.asmedigitalcollection.asme.org/ on 09/30/2016 Terms of Use: http://www.asme.org/about-asme/terms-of-use

local boundary layer is more prone to separation. When the microjets are activated, these shocks disappear as shown in figure 4(b). The boundary layer has been thickened significantly similarly to M=0.3 cases. Consequently, the dynamic stall has been delayed or significantly eliminated as shown by the following two flow sequences (figure 5). We would like to point out that, some (ghost) shadows appear in some of the images shown (mainly in the two lower angle cases) but these do not affect the interpreted results. The appearance of this background noise is the result of having two pinholes placed too close together. The emergence of a very large vortex-like structure is typical of shock-induced separation (figure 5(c)). On the other hand, no vortex or massive separation can be observed if control is used (figures 5(d)-(f)).

Quantitative Analysis

In order to obtain quantitative pressure distribution data, selected images were digitized as described in the experimental setup section. The coordinates where the fringes merge with the airfoil's surface and the corresponding fringe numbers were both recorded. If a boundary layer was clearly discernible, the intersection of the fringe and the outer edge of the boundary layer will be used instead. Using the processed data it was possible to calculate the pressure distribution as a function of chord-wise location (x/c).

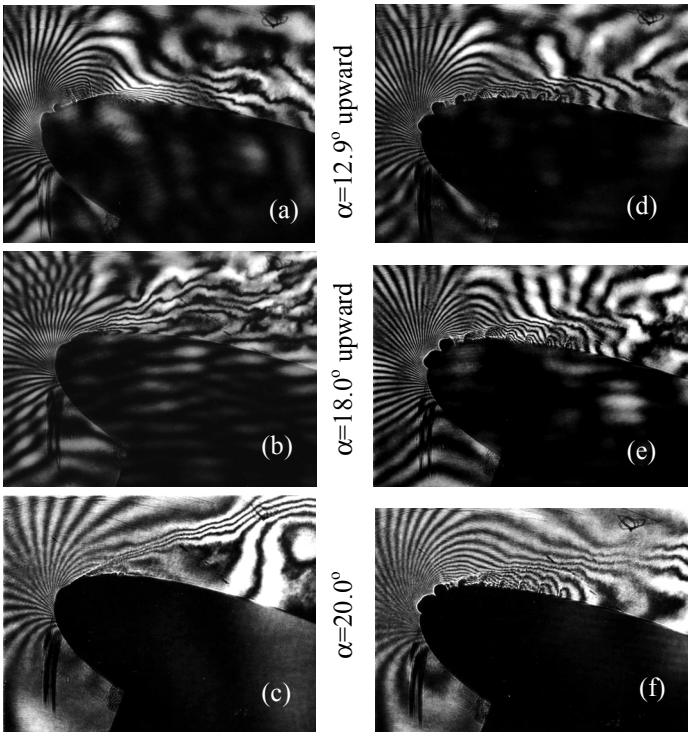

Figure 5. Effect of microjet control on dynamic stall, M=0.4, k=0.05

Figure 6 shows two representative pressure distributions near the leading edge of the airfoil with and without control. The solid symbols present the distribution with no control, while the open symbols follow the distribution with microjet control. Without control, the suction pressure does not fall below –2.0 and there is a large region where the pressure is relatively flat (x/c=0.01 to 0.08). When the control is turned on, the suction pressure re-establishes by reaching to a much lower value of –3.2, indicating that the region is dominated by a locally attached and accelerating flow.

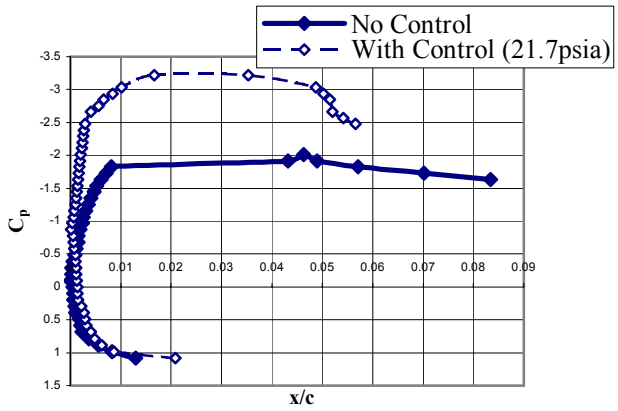

Figure 6 Pressure distribution on leading edge of airfoil, M=0.3, k=0.10, α=16.5° pitching downward

Another measure of the control effectiveness can be represented by determining the minimum pressure coefficient on the upper airfoil's surface. The corresponding variations of the minimum pressure coefficients with and without control as a function of airfoil angle of attack are presented in figure 7. Without control (solid symbols), the minimum pressure initially increases at a relatively constant rate (from an angle of 13° to 16°) and it reaches a lower pressure (-5.0) as the airfoil approaches stall. At this instant, the emergence of a dynamic stall vortex actually induces a low suction pressure near theleading edge to sustain a higher lift. However, as soon as the vortex detaches from the airfoil's nose, this negative pressure peak drops off quickly when massive separation emerges and the airfoil approaches deep stall regime ($\alpha > 16°$). The lowest negative pressure (<-2.0) appears close to when the airfoil reaches to its maximum angle of attack (20°). The recovery of the suction peak is slow. As the airfoil pitches down it reaches a value of approximately –2.5 at an angle of attack of 13°. The large difference of the peak suction before and after the stall indicates that the wing is undergoing a very substantial load fluctuation.

Figure 7 clearly shows the effect that the microjets have on the peak suction pressure. Initially, the peak suction pressure is lower when the control is turned on as expected. The timely release of vorticity through outward blowing means there is an overall reduction of the bounded circulation, which is responsible for the generation of the airfoil's lift.

Before reaching the stall angle, the lift curve with control, while at a slightly lower value compared to that without control, increases about the same rate as the no control case. However, instead of dropping off to lose the suction the controlled wing can maintain its maximum suction pressure for an extended range of angles. At the maximum angle of attack, the peak value of –4.3 is about double that of the corresponding no control case (-2.2). There is no significant drop off with control during pitch-up motion even beyond the stall angle of

Copyright © 2003 by ASME

Downloaded From: http://proceedings.asmedigitalcollection.asme.org/ on 09/30/2016 Terms of Use: http://www.asme.org/about-asme/terms-of-use

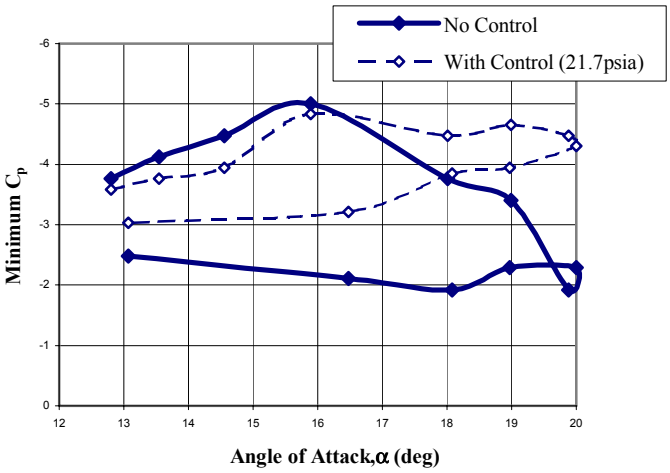

Figure 7 Peak suction pressure coefficient as a function of angle of attack, M=0.3, k=0.10, with and without control

attack (from –4.8 to –4.3). The much smaller hysteresis loop of the suction peak pressure means a more stable flow behavior with microjet control. Although not directly relating to the overall lift, the cyclic history of the peak suction pressure suggests that the averaged lift should increase with microjet control. These observations are consistent for the k=0.05 case as well as the cases at M=0.4.

CONCLUSION

In summary, the microjet control has been shown to be very effective in controlling the dynamic stall process by the use of the PDI technique, both qualitatively and quantitatively. It is speculated that the emergence of a two-layer structure due to microjet blowing is responsible for the control effectiveness. An outer layer effectively convects vorticity away from the leading edge region to avoid local accumulation of vorticity into the dynamic stall vortex. The merging of separated flow pockets behind these microjets forms a thicker inner layer with high mixing characteristics, allowing the boundary flow to withstand the emergence of a locally adverse pressure gradient. The combination of these effects enables the airfoil to pitch to higher angles of attack without the generation of the dynamic stall vortex and the subsequent massive flow separation. Consequently, suction peak pressure at the leading edge can be maintained for the entire operating range of angles of attack with a more stable flow behavior. Additionally, by stabilizing the flow, it can be used to reduce fluttering noise and the associated flow-induced vibrations. Currently, efforts are being made to document the control effectiveness by using quantitative methods such as unsteady surface pressure measurement. Moreover, the microjet control scheme is also being optimized by varying the microjet pattern, number of microjets used, and size of the micro nozzles.

ACKNOWLEDGMENTS

This work was supported by a grant from NASA Ames, monitored by Dr. G. Yumauchi; we are grateful for this support. We would like to thank Dr. P.B. Martin for his help in conducting some of the tests. We also thank additional support and technical advices provided by Dr. C. Tung of US Army Aeroflightdynamics Division and Dr. J.C. Ross and Dr. R.D. Mehta for allowing the use of the FML CDSF.

REFERENCES

1. Van Dommelen, L., and Shen, S.F., "The Spontaneous Generation of the Singularity in a Separating Laminar Boundary Layer," Journal of Computational Physics, Vol. 38, Nov.-Dec., 1980, pp. 125-140.
2. Shih, C., Lourenco, L.M. and Krothapalli, A., "Investigation of Flow at Leading and Trailing Edges of Pitching-Up Airfoil," AIAA Journal, Vol. 33, No. 8, pp. 1369-1376, 1995.
3. Wang, S.C., "Control of Dynamic Stall," PhD Dissertation, 1995, Florida State University.
4. Lewington, N.P., Peake, D.J., Henry, F.S., Kokkalis, A. and Perry, J., "The Application of Air-Jet Vortex Generators to Control the Flow on Helicopter Rotor Blades," private communication.
5. Shih, C., Lou, H., Alvi, F.S., and Krothapalli, A., "Microjet Control of Supersonic Impinging Jets - Control Strategy and Physical Mechanisms," AIAA Paper 2002-6009, 2002 Biennial International Powered Lift Conference, Nov. 2002, Williamsburg, Virginia
6. Chandrasekhara, M.S., Carr, L.W., and Wilder, M.C., "Interferometric Investigations of Compressible Dynamic Stall over a Transiently Pitching Airfoil," AIAA Journal, Vol. 32, No. 3, March 1994.
7. Chandrasekhara, M.S., and Carr, L.W., "Compressibility Effects on Dynamic Stall of Oscillating Airfoils," AGARD-CP-552, pp. 3.1-3.15, Aug. 1995.
8. Tung, C, Chandrasekhara, M.S., "Review of Compressible Dynamic Stall Control Methods," Heli Japan, November 11-13, 2002, Tochigi, Japan.
9. Chandrasekhara, M.S., Wilder, M.C., and Carr, L.W., "Reynolds Number Influence on 2-D Compressible Dynamic Stall," AIAA Paper 96-0073, Jan. 1996, Reno, NV.
10. Carr, L.W. and Chandrasekhara, M.S., "Design and Development of a Compressible Dynamic Stall Facility," Journal of Aircraft, Vol. 29, No. 3, May-June 1992, pp. 314-318.

Copyright © 2003 by ASME

Downloaded From: http://proceedings.asmedigitalcollection.asme.org/ on 09/30/2016 Terms of Use: http://www.asme.org/about-asme/terms-of-use